Brazilian Journal of Physics (2018) 48:576–584
https://doi.org/10.1007/s13538-018-0606-4

CONDENSED MATTER

Multisoliton Dynamics in the Sine-Gordon Model with Two Point Impurities

Evgeniy G. Ekomasov[1,2] · Azamat M. Gumerov[1] · Roman V. Kudryavtsev[1,3] · Sergey V. Dmitriev[4,5] · Vladimir N. Nazarov[3]

Received: 27 June 2018 / Published online: 11 October 2018

Abstract

Collective variables method is used to derive a set of differential equations to describe the dynamics of a kink in the sine-Gordon model with two identical point impurities taking damping into account. It is shown that the scenarios of kink interaction with the waves localized on the impurities, found from the reduced model, are similar to those obtained earlier by numerical integration of the continuous sine-Gordon equation. For the case of the kink passage through the region with the impurities, the structure and properties of the arising on impurities long-lived four-kink multisolitons are analyzed. For the approximate analytical description of the two bound impurity-localized nonlinear waves, the system of differential equations for harmonic oscillators with elastic link is obtained. The analytical model qualitatively reproduces the results of the sine-Gordon equation numerical simulation. The cases of large and small distances between impurities are analyzed. The results of our study uncover new features of the kink-impurity interaction which is important for a number of applications where the sine-Gordon model is used.

Keywords Kink · Soliton · Multisoliton · Sine-Gordon equation · Impurity · Perturbation · Collective variables

1 Introduction

Although solitons initially appeared in the studies of integrable systems, very soon the solitary waves in non-integrable systems became a hot topic because they describe many physical phenomena in hydrodynamics, condensed matter physics, field theory, etc. [1–3]. For example, the sine-Gordon (SGE) equation, which is an integrable partial differential equation, is one of the paradigms in the theory of solitons. It is a fundamental model in many areas of physics. For instance, the sine-Gordon solitons describe the domain walls in magnetics, dislocations in crystals, fluxons in superconducting Josephson junctions and crossings, etc. [4]. Integrable models describe real physical systems only with certain approximation [4] and it is very important to study the sine-Gordon equation taking into account the perturbations arising in particular applications. Various types of perturbations can noticeably influence the soliton dynamics. A great number of works have been dedicated to the study of spatially dependent perturbations in the sine-Gordon model [5–43]. The effect of small perturbations on the SGE solution dynamics can be analyzed in frame of a well-developed perturbation theory (see, e.g., [1, 2, 5–8]), while the case of large

✉ Evgeniy G. Ekomasov
ekomasoveg@gmail.com

Azamat M. Gumerov
article@solitonlab.com

Roman V. Kudryavtsev
xc.89@mail.ru

Sergey V. Dmitriev
dmitriev.sergey.v@gmail.com

Vladimir N. Nazarov
nazarovvn@gmail.com

1 Bashkir State University, Zaki Validi St., 32, Ufa, Russia 450076

2 National Research South Ural State University, Lenina prospect 76, Chelyabinsk, Russia 454080

3 Subdivision of the Ufa Federal Research Centre of the Russian Academy of Sciences, Institute of Molecule and Crystal Physics, 151 Prospekt Oktyabrya, Ufa, Russia 450075

4 Institute for Metals Superplasticity Problems of the Russian Academy of Sciences, Khalturina St. 39, Ufa, Russia 450001

5 National Research Tomsk State University, Lenin Ave. 36, Tomsk, Russia 634050

perturbations is usually treated with the help of numerical methods (see, e.g., [5, 7, 16]). In Refs. [30, 33], the authors have shown the existence of an internal (shape) mode of the sine-Gordon kink in the presence of spatially dependent external forces and damping.

Many papers study the effect of spatial modulation of the periodic potential (or presence of impurities in the system) on the SGE solitons dynamics [1, 2, 5–7, 13–19]. The SGE model with impurities describes, for example, multilayer ferromagnet [40–43]. The importance of the impurity modes in the kink dynamics has been shown in [5, 14–19, 34]. The structure and properties of localized nonlinear waves excited on an impurity were analyzed numerically in [26–29]. The case of several delta-shaped point impurities, which are of interest in some physical applications [44], and even the case of a spatially modulated harmonic potential [25] were considered. The possibility of excitation of a kink-impurity mode as a result of kink interaction with an impurity has also been considered, and a considerable change in the kink dynamics after the interaction has been reported [5, 6, 16].

SGE kinks have received a lot of attention from the researchers, while it is much less known about multisoliton solutions (see, e.g., [27, 45–51]). Earlier [45, 46], an interesting three-kink wobble type SGE solution was found. In [27], it was shown that such SGE solution can be excited at a kink pinned by an attractive impurity. In the case of two identical impurities, which models a five-layer ferromagnet, strong collective effects in the system were revealed in the absence of damping [40, 47, 48]. For instance, in such structures, SGE multisolitons can be excited and a particular type of four-kink multisoliton was studied. Additionally, another interesting effect of quasi-tunneling was revealed, in which a kink passing through a double impurity needs less kinetic energy than for passing a single impurity of the same sizes. All the results mentioned above were obtained using numerical methods, while it is desirable to solve the problem of the kink interaction with two impurities using analytical methods, for example, the collective variables method.

In this paper, the interaction of SGE kink with nonlinear waves localized on two identical point impurities is considered. Using the collective variables method, taking damping into account, a set of differential equations that describes the dynamics of the kink center and the waves localized on the impurities is derived. Possible scenarios for the kink interaction with localized waves are analyzed. For the case of the kink passage through the region with the impurities, the structure and dynamics of four-kink solitons excited on impurities are studied using both the reduced set of equations and numerical calculations for the continuum SGE model.

2 Main Equations and Results of Kink Dynamics in the Model with Two Impurities

Let us consider a system defined by the Lagrangian

$$L=\int_{-\infty}^{+\infty}\left\{\frac{1}{2}u_t^2-\frac{1}{2}u_x^2-[1-\varepsilon\delta(x)-\varepsilon\delta(x-d)](1-\cos u)\right\}dx, \quad (1)$$

where the term $\varepsilon\delta(x)$ simulates a point impurity, $\delta(x)$ is Dirac delta function, and ε is a constant. Rayleigh dissipation function has the form

$$R=\int_{-\infty}^{+\infty}\frac{1}{2}\alpha u_t^2 dx\ , \quad (2)$$

where α is the damping parameter. The Lagrangian (1) corresponds to the equation of motion for a scalar field $u(x,t)$ in the form

$$u_{tt}-u_{xx}+\sin u=[\varepsilon\delta(x)+\varepsilon\delta(x-d)]\sin u-\alpha u_t, \quad (3)$$

where the damping (2) is taken into account. Equation (3) is the modified sine-Gordon equation (MSGE) considered here. The perturbation terms in the right-hand side of Eq. (3) describe, for example, the five-layer ferromagnet with different values of the magnetic anisotropy ε in different layers [41, 42]. Equation (3) has, for the zero right-hand side, a solution in the form of a kink

$$u_0=4\arctan e^{x-x(t)}, \quad (4)$$

where $x(t)$ is the kink center coordinate. On the other hand, Eq. (3) with zero right-hand side has a spatially localized solution in the form of resting breather [1, 2].

$$u(x,t)=4\arctan\left[\frac{\sqrt{1-\Omega^2}}{\Omega}\frac{\sin\ (\Omega t)}{\cosh\ \left((x-x_0)\sqrt{1-\Omega^2}\right)}\right], \quad (5)$$

where Ω is breather frequency and x_0 is the coordinate of its center. Let us study the kink dynamics with regard to the excitation of localized waves on the impurities. For the theoretical analysis of the structure and dynamics of Eq. (3) solutions, it is possible to use an approximate collective coordinate approach previously applied to the analysis of the impurity mode oscillation at a single point impurity [1, 2]. The presence of waves localized on the two impurities (or impurity modes) is taken into account through the introduction of two collective variables, $a_1 = a_1(t)$ and $a_2 = a_2(t)$, which are the amplitudes of these waves. The expressions for the impurity modes will be taken in the form similar to that used previously for the case of single impurity [1, 5].

$$\begin{cases} u_1=a_1(t)\exp(-\varepsilon|x|/2)\ , \\ u_2=a_2(t)\exp(-\varepsilon|x-d|/2). \end{cases} \quad (6)$$

In the small-amplitude oscillations approximation, assume that $a_n(t) = a_{n0}\cos(\Omega t + \theta_0)$, where θ_0 is the initial phase. When solving (3) for the case of single impurity, the following expression for the impurity mode frequency can be obtained $\Omega = (1 - \varepsilon^2/4)^{1/2}$. The general solution of the problem, u, will be searched in the form:

$$u = u_0 + u_1 + u_2 \tag{7}$$

Suppose that $\dot{x}(t)$, $a_n(t)$, and $_n(t)$ are sufficiently small (of the order of ε), i.e., the impurity modes with small amplitudes are excited at a slowly moving kink. In the framework of this approximation, we consider

$$u_n \ll u_0 \tag{8}$$

Then the nonlinear terms in the Lagrangian (1) can be expanded in the Taylor series up to the second-order terms in ε [2].

$$\cos(u_0 + u_1 + u_2) \approx \cos u_0 - (u_1 + u_2)\sin u_0 - \frac{(u_1 + u_2)^2}{2}\cos u_0 \tag{9}$$

Substituting (7) into (1) based on the approximation (9) leads after integration to a new effective Lagrangian, dependent on new variables $x(t)$, $a_1(t)$, and $a_2(t)$,

$$\begin{aligned} L \approx\, & 4\dot{x}^2(t) + \left[\dot{a}_1^2(t) + \dot{a}_2^2(t) + 2\dot{a}_1(t)\dot{a}_2(t)E\right]/\varepsilon - 2U_1(x(t)) \\ & -2U_2(x(t)) + 2a_1(t)\left[F_1(x(t)) + F_2(x(t))e^{-\varepsilon d/2}\right] \\ & +2a_2(t)\left[F_1(x(t))e^{-\varepsilon d/2} + F_2(x(t))\right] \\ & +a_1^2(t)\left[-\Omega^2/\varepsilon + \varepsilon e^{-\varepsilon d}/2 + U_1(x(t)) + U_2(x(t))e^{-\varepsilon d}\right] \\ & +a_2^2(t)\left[-\Omega^2/\varepsilon + \varepsilon e^{-\varepsilon d}/2 + U_1(x(t))e^{-\varepsilon d} + U_2(x(t))\right] \\ & +2a_1(t)a_2(t)\left[\varepsilon/2 - E\Omega^2 e^{\varepsilon d/2}/\varepsilon + U_1(x(t)) + U_2(x(t))\right]e^{-\varepsilon d/2}, \end{aligned} \tag{10}$$

where

$$\begin{aligned} E &= (1 + \varepsilon d/2)e^{-\varepsilon d/2}, \Omega^2 = 1 - \varepsilon^2/4, U_1(x(t)) \\ &= -\varepsilon/\cosh^2(x(t)), U_2(x(t)) \\ &= -\varepsilon/\cosh^2(x(t) - d), F_1(x(t)) \\ &= \varepsilon\sinh(x(t))/\cosh^2(x(t)), F_2(x(t)) \\ &= \varepsilon\sinh(x(t) - d)/\cosh^2(x(t) - d) \end{aligned} \tag{11}$$

Similarly integrating (2) for the effective Rayleigh function we obtain

$$R = \alpha\left[4\dot{x}^2(t) + \left[\dot{a}_1^2(t) + \dot{a}_2^2(t) + 2\dot{a}_1(t)\dot{a}_2(t)E\right]/\varepsilon\right] \tag{12}$$

The equations of motion for $x(t)$, $a_1(t)$, and $a_2(t)$ can be obtained by inserting the effective Lagrangian (10) and Rayleigh function (12) into the Lagrange system of equations of the second order

$$\begin{aligned} 4\left[\ddot{x}(t) + \alpha\dot{x}(t)\right] = & -U_1'(x(t)) - U_2'(x(t)) \\ & + a_1(t)\left[F_1'(x(t)) + F_2'(x(t))e^{-\varepsilon d/2}\right] \\ & + a_2(t)\left[F_1'(x(t))e^{-\varepsilon d/2} + F_2'(x(t))\right] \\ & + a_1^2(t)\left[U_1'(x(t)) + U_2'(x(t))e^{-\varepsilon d}\right]/2 \\ & + a_2^2(t)\left[U_1'(x(t))e^{-\varepsilon d} + U_2'(x(t))\right]/2 \\ & + a_1(t)a_2(t)\left[U_1'(x(t)) + U_2'(x(t))\right]e^{-\varepsilon d/2} \end{aligned} \tag{13}$$

$$\begin{aligned} & \left[\ddot{a}_1(t) + \alpha\dot{a}_1(t) + a_1(t)\Omega^2\right]\left(1 - E^2\right)/\varepsilon \\ & \quad = F_1(x(t))\left(1 - Ee^{-\varepsilon d/2}\right) - F_2(x(t))\varepsilon d/2e^{-\varepsilon d/2} \\ & \quad + a_1(t)\left[-\varepsilon^2 d/4e^{-\varepsilon d} + U_1(x(t))\left(1 - Ee^{-\varepsilon d/2}\right) - U_2(x(t))\varepsilon d/2e^{-\varepsilon d}\right] \\ & \quad + a_2(t)\left[\left(1 - Ee^{-\varepsilon d/2}\right)\varepsilon/2 + U_1(x(t))\left(1 - Ee^{-\varepsilon d/2}\right) - U_2(x(t))\varepsilon d/2\right]e^{-\varepsilon d/2} \end{aligned} \tag{14}$$

$$\begin{aligned} & \left[\ddot{a}_2(t) + \alpha\dot{a}_2(t) + a_2(t)\Omega^2\right]\left(1 - E^2\right)/\varepsilon \\ & \quad = F_2(x(t))\left(1 - Ee^{-\varepsilon d/2}\right) - F_1(x(t))\varepsilon d/2e^{-\varepsilon d/2} \\ & \quad + a_2(t)\left[-\varepsilon^2 d/4e^{-\varepsilon d} + U_2(x(t))\left(1 - Ee^{-\varepsilon d/2}\right) - U_1(x(t))\varepsilon d/2e^{-\varepsilon d}\right] \\ & \quad + a_1(t)\left[\left(1 - Ee^{-\varepsilon d/2}\right)\varepsilon/2 + U_2(x(t))\left(1 - Ee^{-\varepsilon d/2}\right) - U_1(x(t))\varepsilon d/2\right]e^{-\varepsilon d/2}. \end{aligned} \tag{15}$$

From the resulting set of equations, in the limiting case $d \to \infty$, we can obtain the already known equations for the case of kink motion in a model with one impurity [5]. First, we shall consider the effect of two impurities on kink dynamics. In the calculations, it is assumed that at the time $t = 0$ the kink is at relatively large distance from the impurities, $x(0) = -20$, and it moves toward them with the initial velocity $\dot{x}(0)$, while the impurity modes are not excited, $a_1(0) = {}_1(0) = a_2(0) = {}_2(0) = 0$. In Fig. 1, possible kink dynamics are presented for different initial velocities and distances between impurities as described in the caption. The following scenarios are shown: the kink is captured in the region of the first (curve 3) or second (curve 2) impurity; the kink oscillates between two impurities for a long time (curve 1); the kink is reflected from the impurity region and starts to move in the opposite direction (curve 5), or passes through the impurity region (curve 4). In the last two cases, oscillating localized high-amplitude nonlinear

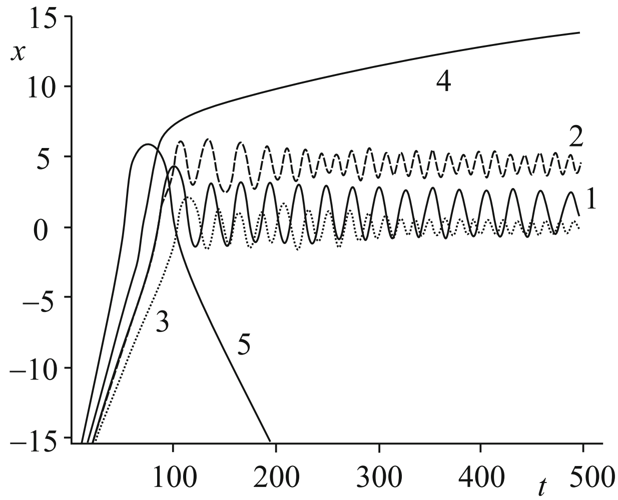

Fig. 1 Dependence of the kink center coordinate on time $x(t)$, calculated from (13)–(15) with $\varepsilon = 0{,}7$, $\alpha = 0.002$, $x(0) = -20$, $a_1(0) = {}_1(0) = a_2(0) = {}_2(0) = 0$ and $\dot{x}(0) = 0.24$, $d = 2$ (curve 1); $\dot{x}(0) = 0.24$, $d = 4.5$ (curve 2); $\dot{x}(0) = 0.20$, $d = 6$ (curve 3); $\dot{x}(0) = 0.29$, $d = 4$ (curve 4); $\dot{x}(0) = 0.4$, $d = 3.1$ (curve 5)

waves of breather type are excited on the impurities, which significantly affect the dynamics of the kink. Firstly, a considerable part of the kink initial energy can be spent on their excitation. Secondly, the subsequent interaction of the kink with these waves localized on the impurities can result in resonance effects (for example, in the case of single impurity, reflection from the attractive potential can be observed for some parameters [5, 16, 28]). We can also highlight the case when the impurities are located close enough to each other, then the energy necessary for the transition between them is small and the kink can oscillate between them for a long time (see curve 1 in Fig. 1).

Note that using numerical methods for solving Eq. (3), all possible scenarios of kink motion described above were obtained both for the case of point and extended impurities [40, 47]. From here, it follows that for our case of two identical impurities, using the method of collective variables, one can obtain all basic variants of the kink interaction with impurities that were observed earlier in the numerical simulation of MSGE (3).

3 Dynamics of the Multisoliton Waves

3.1 Analytical Results

Let us consider the structure and dynamics of nonlinear waves localized on the point impurities excited, for example, as a result of the kink scattering on the impurities. To obtain from the system of Eqs. (13)–(15) for describing the dynamics of two impurity modes in the absence of kink and damping, we assume that $x(t) \to \infty$ and $\alpha = 0$. Then the two equations for the variables $a_1(t)$ and $a_2(t)$ assume the form:

$$\left[\ddot{a}_1(t) + a_1(t)\Omega^2\right]\left(1 - E^2\right)/\varepsilon$$
$$= -a_1(t)\varepsilon^2 d/4e^{-\varepsilon d} + a_2(t)\left(1 - Ee^{-\varepsilon d/2}\right)\varepsilon/2e^{-\varepsilon d/2}, \quad (16a)$$
$$\left[\ddot{a}_2(t) + a_2(t)\Omega^2\right]\left(1 - E^2\right)/\varepsilon$$
$$= -a_2(t)\varepsilon^2 d/4e^{-\varepsilon d} + a_1(t)\left(1 - Ee^{-\varepsilon d/2}\right)\varepsilon/2e^{-\varepsilon d/2}. \quad (16b)$$

The set of Eq. (16) for $a_1(t)$ and $a_2(t)$ can be written in a shorter form with the use of the following notations

$$F = F(\varepsilon, d) = \frac{\varepsilon^2}{2}\frac{1 - (1 + \varepsilon d/2)e^{-\varepsilon d}}{1 - (1 + \varepsilon d/2)^2 e^{-\varepsilon d}} e^{-\frac{\varepsilon d}{2}}, \quad (17)$$

$$\Omega_0^2 = \Omega_0^2(\varepsilon, d) = 1 - \frac{\varepsilon^2}{4} - \frac{\varepsilon^2}{2}\frac{\left(1 + e^{-\varepsilon d/2}\right)e^{-\varepsilon d/2}}{1 + (1 + \varepsilon d/2)e^{-\varepsilon d/2}} \quad (18)$$

Using (17) and (18), multiplying both Eq. (16) by $\varepsilon[1 - E^2]^{-1}$, we obtain

$$\begin{cases} \ddot{a}_1(t) + a_1(t)\Omega_0^2 = [a_2(t) - a_1(t)]F \ , \\ \ddot{a}_2(t) + a_2(t)\Omega_0^2 = [a_1(t) - a_2(t)]F \ . \end{cases} \quad (19)$$

The system (19) is a set of two ordinary differential equations of the second order. It follows from (19) that the breather type waves localized on the impurities, in the small-amplitude approximation, can be described by a system of two coupled effective harmonic oscillators with the same proper frequency $\Omega_0(\varepsilon,d)$. Each of them is under external force $(a_2(t) - a_1(t))F(\varepsilon,d)$ (of elastic type) from the other oscillator. In this case, the coupling coefficient $F(\varepsilon,d)$ can vary, for example, by changing parameter d, which is the distance between impurities. Let us analyze the behavior of functions (17) and (18) in the limiting case $d \to \infty$,

$$\lim_{d\to\infty} F(\varepsilon, d) = 0, \quad (20)$$

$$\lim_{d\to\infty} \Omega_0^2(\varepsilon, d) = 1 - \frac{\varepsilon^2}{4} = \Omega^2. \quad (21)$$

Expression (20) shows that with the parameter d increase, the coupling coefficient vanishes, and (19) goes into the equations describing uncoupled harmonic oscillators. From (21), one can see that frequency Ω_0 in the limit $d \to \infty$ assumes the value for a single impurity. In this case, the oscillators move independently at the proper frequency of single impurity.

Let us study the dependence of expressions (17) and (18) on the parameter d. Figure 2 shows that at $d \to \infty$, both functions Ω_0 and F asymptotically tend to the corresponding values given by (21) and (20), respectively. In the limit, $d \to 0$ function F sharply increases, which corresponds to the increase of the

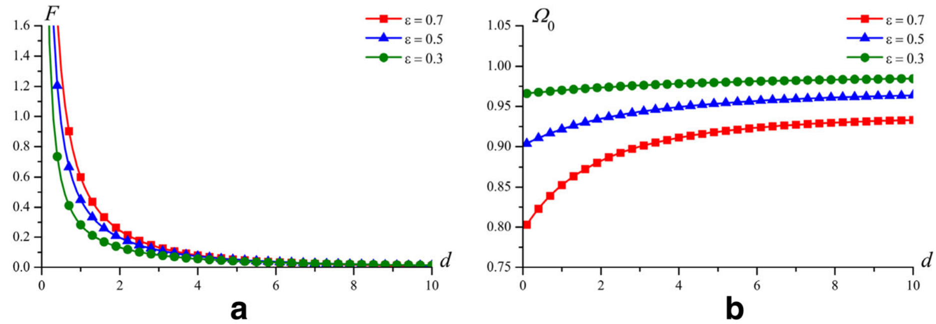

Fig. 2 The dependence of parameters of the systems (20) and (21) on the distance between impurities d: **a** $F(\varepsilon,d)$; **b** $\Omega_0(\varepsilon,d)$

bond rigidity between the effective oscillators. On the other hand, $\Omega_0(\varepsilon,d=0)$ in this limit approaches the finite value corresponding to the duplicated effective oscillator, i.e., in the expression for Ω one has to insert the value 2ε.

As it is known, the system of the two elastically coupled harmonic oscillators may have solutions in the form of in-phase or antiphase oscillations. To analyze properties of these solutions, let us introduce the new variables:

$$\varphi_S = \frac{a_1(t) + a_2(t)}{\sqrt{2}} \quad , \quad \varphi_A = \frac{a_1(t) - a_2(t)}{\sqrt{2}} \tag{22}$$

By adding and subtracting equations in the system (19) and using (22), one can come to the following set of equations

$$\begin{cases} \ddot{\varphi}_S + \Omega_S^2 \varphi_S = 0, \\ \ddot{\varphi}_A + \Omega_A^2 \varphi_A = 0, \end{cases} \tag{23}$$

where $\Omega_S = \Omega_0$, $\Omega_A = (\Omega_0 + 2F)^{1/2}$. Thus, the oscillations described by (19) can be regarded as a superposition of oscillations with symmetric Ω_S and anti-symmetric Ω_A modes, which are commonly referred to as normal frequencies (modes) of the system, and variables (22) are called normal coordinates. In special cases, when the oscillations are in phase or antiphase, the whole system, and each oscillator in particular, oscillate at the corresponding normal frequency. For clarity, let us consider a few special cases with specially selected initial conditions. For example, at time $t = 0$ both effective oscillators deflect from their equilibrium positions on a_{0S} and have the same speed υ_{0S}. In this case, the movement will be symmetrical (the effective elastic bond is not stretched) and given by the following expression:

$$a_1(t) = a_2(t) = a_{0s}\cos\Omega_S t + \frac{\dot{a}_{0s}}{\Omega_S}\sin\Omega_S t \tag{24}$$

If at $t = 0$, both effective oscillators are deviated by a_{0A} in different directions and have the same speed υ_{0A}, then the anti-symmetric vibrations are excited:

$$a_1(t) = -a_2(t) = a_{0a}\cos\Omega_A t + \frac{\dot{a}_{0a}}{\Omega_A}\sin\Omega_A t \tag{25}$$

At an arbitrary choice of the initial conditions, motion of the system is described by a superposition of (24) and (25):

$$\begin{cases} a_1(t) = a_{0s}\cos\Omega_S t + \dfrac{\dot{a}_{0s}}{\Omega_S}\sin\Omega_S t + a_{0a}\cos\Omega_A t + \dfrac{\dot{a}_{0a}}{\Omega_A}\sin\Omega_A t, \\ a_2(t) = a_{0s}\cos\Omega_S t + \dfrac{\dot{a}_{0s}}{\Omega_S}\sin\Omega_S t - a_{0a}\cos\Omega_A t - \dfrac{\dot{a}_{0a}}{\Omega_A}\sin\Omega_A t. \end{cases} \tag{26}$$

Solution (26) can be obtained by solving Eq. (23), while returning to the original variables (22).

3.2 Numerical Results

Let us consider possible dynamics of system (19) by means of numerical integration with the use of the fourth-order Runge-Kutta method for different initial conditions. Let us analyze the type of oscillations depending on parameter d and initial conditions. This will allow to test the correctness and accuracy of calculation of the characteristic frequencies using the numerical method, and to address the issue related to frequency determination. To do so, we assume for simplicity $\dot{a}_1$ $(t = 0) = 0$; $\dot{a}_2$ $(t = 0) = 0$, and vary only $a_1(t = 0) = a_{01}$ and $a_2(t = 0) = a_{02}$. Next, let us consider three cases corresponding to different initial conditions. We use Fourier-decomposition to identify frequencies Ω_S and Ω_A.

The results of numerical simulation are shown in Fig. 3 for the time evolution of a_1 and a_2 and for Fourier analysis of these signals. Initial conditions are listed in the caption. The initial conditions are chosen so that the case in Fig. 3a is close to the phase oscillations, so the amplitude of the first frequency component in the Fourier spectrum is significantly higher than that of the second component. Here, we can say that, in this motion, symmetric summands of superposition (26) are dominating. Another situation is observed in Fig. 3c, where anti-symmetric summands are dominating. Thus, in particular cases, when the oscillations are very close to either symmetric or anti-symmetric cases, there can appear a problem with definition of one of the frequency components. Therefore, for the frequency components analysis, the best case is similar to that shown in Fig. 3b with nearly equal contribution from symmetrical and anti-symmetric summands. In addition, the

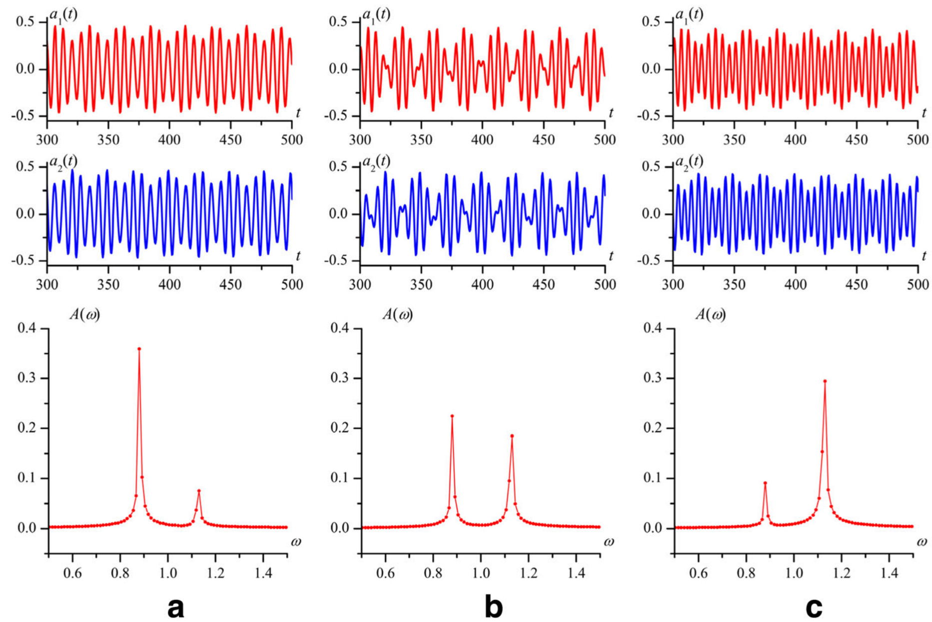

Fig. 3 Time evolution of the deviations from the equilibrium position of the first $a_1(t)$ and second $a_2(t)$ oscillator, resulting from numerical solution of (19) and corresponding discrete Fourier expansion $A(\omega)$ of $a_1(t)$. Parameters: $\varepsilon = 0.7$, $d = 2$. Initial conditions: **a** $a_{01} = 0.5$, $a_{02} = 0.3$, **b** $a_{01} = 0.5$, $a_{02} = 0$, **c** $a_{01} = 0.5$, $a_{02} = -0.3$

calculated frequencies show good quantitative agreement with analytical expressions for Ω_S and Ω_A.

Next, we consider the effect of parameter d that controls the stiffness of the effective bond between oscillators (see Fig. 2a), on the emerging oscillation modes. As an example, we present the results obtained only for the case $\varepsilon = 0.7$. The calculations show that other considered cases are similar to this one. Let us introduce in the initial conditions the initial phase difference of the oscillators in order to excite the beating oscillations. Figure 4 shows three different cases corresponding to different values of the parameter $d = \{0.3, 1, 3\}$, which by the nature of frequency spectra $A(\omega)$ can be (conditionally) assigned to different oscillation modes.

For a short distance between the impurities, $d = 0.3$ (Fig. 4a), it is clear that the link is very hard. For any initial conditions, the oscillation phase difference reduces in time to zero, and after a transient period, the oscillators begin to move in phase at a single frequency. The anti-symmetric mode is unstable and it cannot be realized. In the case of moderate distances between the impurities, $d = 1$ (Fig. 4b), the link is of medium hardness and this results in strong beating of oscillations. Frequency components in the spectrum $A(\omega)$ are located

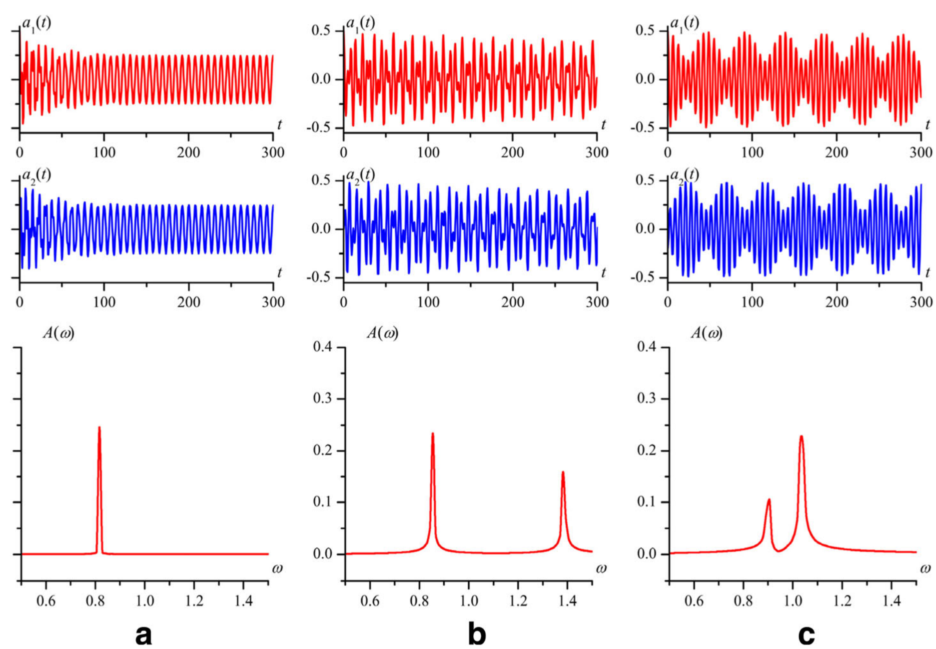

Fig. 4 Time evolution of the deviations from the equilibrium position of the first $a_1(t)$ and second $a_2(t)$ oscillator, resulting from numerical solution of (19) and corresponding discrete Fourier expansion $A(\omega)$ of $a_1(t)$. Parameters: $\varepsilon = 0.7$, **a** $d = 0.3$, $a_{01} = 0.5$, $a_{02} = 0$; **b** $d = 1$, $a_{01} = 0.5$, $a_{02} = 0$; **c** $d = 3$, $a_{01} = 0.5$, $a_{02} = -0.2$

far from each other. From Fig. 4c, for the case of large distance between impurities, $d = 3$, one can see that the link is weak, and oscillation beating is weak. Frequency components in the spectrum $A(\omega)$ are located much closer. This oscillation mode corresponds to the weak bond case (see, e.g., [52, 53]), and general solution (26) can be simplified for it.

4 Dynamics of the Multisoliton Waves: Numerical Results

To check the domain of applicability of the analytical model and set of Eq. (19), obtained by perturbation theory for solitons (collective coordinate method), let us investigate numerically the structure and dynamics of localized nonlinear waves by solving the original Eq. (3). To date, quite a number of methods have been developed for the numerical solution of such nonlinear differential equations. For example, a number of studies [54, 55] use spectral and pseudospectral Fourier methods for solving SGE. In the work [56], a compact finite-difference scheme and DIRKN-method were used. The method of lines is used in [57]. In this paper, the finite differences method is used for the numerical solution of Eq. (3). We select a three-layer explicit scheme with approximation of derivatives on a five-point pattern of the "cross" type. It was previously applied to simpler SGE modifications (see for example [7, 26]). Let Δx be the coordinate step and τ be the time step. This numerical scheme of the second approximation order at Δx and τ has conditional stability when $(\tau/\Delta x) \leq 1/2$. In addition, the scheme used is rather flexible and it can be with minimal changes adapted both for other modifications of one-dimensional Eq. (3), and for multidimensional SGE variants.

The numerical algorithm to integrate Eq. (3) works as follows. At the time $t = 0$, we have SGE kink of the form

$$u_0(x,t) = 4\arctan\left[\exp\left(\pm\gamma(x - x(t))\right)\right] \tag{27}$$

where $\gamma = (1 - v^2)^{-1/2}$, v is the kink velocity, $x(t) = vt + x_0$ is the kink center coordinate. The boundary conditions are as follows: $u(-\infty, t) = 0$, $u(+\infty, t) = 2\pi$, $u'(\pm\infty, t) = 0$. Using the grid of $N = 10^4$ points, taking time as an iterative parameter and following the conditions of the explicit scheme convergence, the value of the function $u(x,t)$ in the next time step was calculated. From the found function $u(x,t)$, we obtain the main characteristics of the nonlinear wave. Numerical experiment show that after the kink passage through the impurities, the nonlinear waves are excited on each impurity, and those waves are well described by the oscillating bell-shaped functions $u(x,t)$. For the case of one attractive impurity, there has been shown previously [26] that the localized nonlinear wave can be regarded as a resting breather, which is a bound kink-antikink state. The amplitude of the excited breather depends on the kink initial velocity. The breather oscillation frequency ω_{breather} practically does not depend on the kink velocity and is determined by the impurity parameters. In the case of two impurities, the excited localized impurity modes interact with each other, that is why the resulting MSGE solution can be called a four-kink multisoliton.

Let us calculate frequency dependences of the localized impurity waves depending on the distance between the impurities. Since the localized waves are excited by the kink passage, the initial kink velocity v_0 determines initial phase difference between the localized waves. It is important to note that it is impossible to set an arbitrary initial oscillations phase difference by changing v_0. Consequently, it is impossible to excite the entire spectrum of possible states. For example, it is not always possible to excite anti-symmetric oscillation modes.

The solid lines in Fig. 5 plot the analytically calculated symmetric (curve 2) and antisymmetric (curve 1) mode frequencies of the system (19) as the functions of the parameter d. The symbols show the same for the symmetric (curve 4) and antisymmetric (curve 3) fluctuations of the MSGE breathers. These frequency components were calculated using the Fourier analysis method described above. The results presented in Fig. 5 suggest that there is qualitative agreement

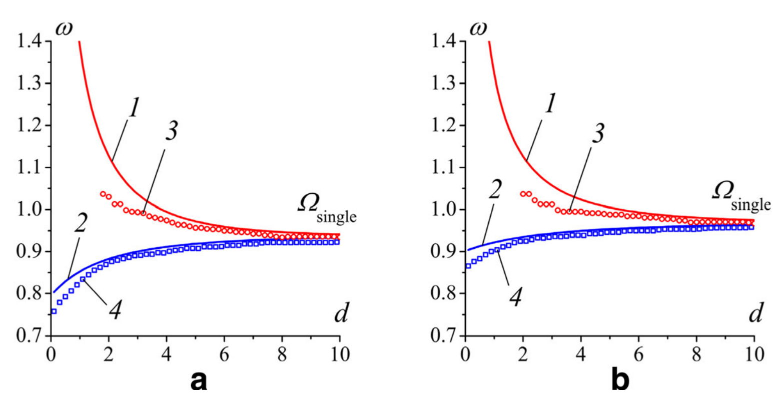

Fig. 5 Possible values of the localized waves oscillation frequencies depending on the distance between the impurities d for: **a** $\varepsilon = 0.5$ and **b** $\varepsilon = 0.7$. Curve 1 is for the in-phase oscillation frequency Ω_S ($a_{02} = 0.5$), curve 2 is for the antiphase oscillation frequency Ω_A ($a_{02} = -0.5$), symbols 3 is MSGE localized waves in-phase oscillation frequency, symbols 4 is MSGE localized waves antiphase oscillation frequency

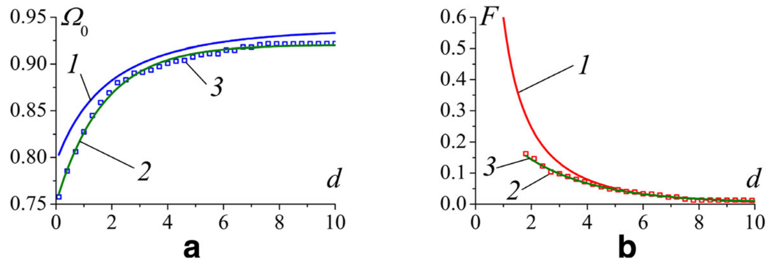

Fig. 6 The dependence of the parameters **a** $\Omega_0(\varepsilon,d)$ and **b** $F(\varepsilon,d)$ on the distance between the impurities d at $\varepsilon = 0.7$. Curve 1 is calculated by analytical expressions **a** (17) and **b** (18), symbols 2 were obtained by numerical simulation of the MSGE localized waves, curve 3 is the approximation of the numerically obtained data by expression (28): **a** $A = 0.92048$, $B = -0.16906$, $C = -0.5878$; **b** $A = 0.00417$, $B = 0.31079$, $C = -0.39969$

between the analytical and numerical results. The discrepancy between the curves for the small values of d is primarily due to the discrepancy between analytical expressions for $\Omega_0(\varepsilon,d)$ and $F(\varepsilon,d)$ and the results of numerical calculation of the MSGE breathers oscillations (see Fig. 6). Indeed, expressions (17) and (18) describe well the bond between the effective oscillators and their natural frequencies only for relatively large values of d. However, the curves obtained numerically from MSGE can be approximated by a simple exponential dependence (Fig. 6, curves 3) of the form:

$$f(x) = A + Be^{Cx}. \tag{28}$$

Figure 5 represents three qualitatively different parameter regions (similar to the cases considered in Fig. 4).

In the region I ($d < 2$), only the in-phase mode was excited by kink passage. Obviously, the antiphase mode excitation requires much higher interaction energy. In the region II ($2 < d < 4$), there is a strong interaction between the localized impurity waves with periodic energy pumping. In the region III ($d > 4$), the increase of d results in localized impurity waves frequencies asymptotical approach to Ω_{single}. In this region, by changing v_0, one can excite both in-phase and antiphase oscillations. As a fundamental difference between the regions II and III, there can be mentioned the fact that parameter v_0 variation allows to initiate the states which are much closer to a symmetric mode.

5 Conclusions

We have studied the sine-Gordon equation perturbed by the introduction of the two identical delta-shaped impurities and damping, as given by Eq. (3). Using the method of collective variables that takes into account damping, we have derived the set of differential equations describing the dynamics of the kink and the waves localized on the two impurities. We have described analytically the possible scenarios of the kink interaction with the waves localized on the impurities. Our conclusion is that the reduced set of equations makes it possible to describe all the basic scenarios of kink interaction with the two-point impurities, which was confirmed by comparison of the analytical results with the results of numerical simulation of the continuous system.

We have shown that when the kink passes through the impurities, under certain conditions, it can excite the impurities of the long-lived four-kink multisoliton. For the analytical description of the four-kink multisoliton in the form of the two nonlinear waves localized on the impurities, the set of two differential equations for harmonic oscillators coupled via elastic bond has been derived. The analytical model qualitatively describes the results of the numerical simulations for the continuous system.

Our results contribute to a deeper understanding of the kink-impurity interactions in the Klein-Gordon fields which are widely used in a number of physical applications.

Funding The work was supported by Act 211 Government of the Russian Federation, contract № 02.A03.21.0011. For S.V.D., the work was supported by the Russian Science Foundation, grant No. 16-12-10175. The work was partly supported by the State Assignment of IMSP RAS. For A.M.G. and R.V.K., the work was supported by the Russian Foundation for Basic Research, grant No. 18-31-00122.

References

1. O.M. Braun, Y.S. Kivshar, *The Frenkel-Kontorova Model: Concepts, Methods, and Applications* (Springer, Berlin, 2004)
2. T. Dauxois, M. Peyrard, *Physics of Solitons* (Cambridge University Press, New York, 2010)
3. Encyclopedia of Nonlinear Science. Scott A. (Ed.). New York: Routledge (2004)
4. J. Cuevas-Maraver, P.G. Kevrekidis, F. Williams, Editors, The Sine-Gordon Model and its Applications. From Pendula and Josephson Junctions to Gravity and High-Energy Physics, Springer, Heidelberg, New York, Dordrecht, London (2014)
5. F. Zhang, Y.S. Kivshar, L. Vazquez, Resonant kink-impurity interactions in the sine-Gordon model. Phys. Rev. A **45**, 6019–6030 (1992)
6. M.B. Fogel, S.E. Trullinger, A.R. Bishop, J.A. Krumhandl, Dynamics of sine-Gordon solitons in the presence of perturbations. Phys. Rev. B **15**, 1578–1592 (1977)
7. J.P. Currie, S.E. Trullinger, A.R. Bishop, J.A. Krumhandl, Numerical simulation of sine-Gordon soliton dynamics in the presence of perturbations. Phys. Rev. B **15**(12), 5567–5580 (1977)
8. Y.S. Kivshar, B.A. Malomed, Addendum: Dynamics of solitons in nearly integrable systems. Rev. Mod. Phys. **63**(1), 211 (1991)

9. Y.S. Kivshar, B.A. Malomed, F. Zhang, L. Vazquez, Creation of sine-Gordon solitons by a pulse force. Phys. Rev. B **43**, 1098–1109 (1991)
10. J.A. Gonzales, A. Bellorin, L.E. Guerrero, Phys. Rev. E. (Rapid Commun.) **65**, 065601 (2002)
11. R.H. Goodman, P.J. Holmes, M.I. Weinstein, Interaction of sine-Gordon kinks with defects: phase space transport in a two-mode model. Physica D: Nonlinear Phenomena **161**(1), 21–44 (2002)
12. N.R. Quintero, A. Sanchez, F.G. Merten, Existence of internal modes of sine-Gordon kinks. Phys. Rev. E **62**(1), R60–R63 (2000)
13. C.J.K. Knight, G. Derks, A. Doelman, H. Susanto, Stability of stationary fronts in a non-linear wave equation with spatial inhomogeneity. Journal of Differential Equations **254**(2), 408–468 (2013)
14. B. Piette, W.J. Zakrzewski, Scattering of sine-Gordon breathers on a potential well. Phys. Rev. E **79**, 046603 (2009)
15. K. Javidan, Analytical formulation for soliton-potential dynamics. Phys. Rev. E **78**, 046607 (2008)
16. B. Piette, W.J. Zakrzewski, Scattering of sine-Gordon kinks on potential wells. J. Phys. A Math. Theor. **40**, 5995–6010 (2007)
17. R.H. Goodman, R. Haberman, Interaction of sine-Gordon kinks with defects: the two-bounce resonance. Physica D: Nonlinear Phenomena. **195**(3), 303–323 (2004)
18. R.H. Goodman, R. Haberman, Chaotic Scattering and then-Bounce Resonance in Solitary-Wave Interactions. Phys. Rev. Lett. **98**(10), 104103 (2007)
19. B. Piette, W.J. Zakrzewski, Dynamical properties of a soliton in a potential well. J. Phys. A Math. Theor. **40**(2), 329–346 (2007)
20. D. Bazeia, L. Losano, J.M.C. Malbouisson, R. Menezes, Classical behavior of deformed sine-Gordon models. Physica D: Nonlinear Phenomena **237**(7), 937–946 (2008)
21. R. Chacon, A. Bellorín, L.E. Guerrero, J.A. Gonzalez, Spatiotemporal chaos in sine-Gordon systems subjected to wave fields: onset and suppression. Phys. Rev. E **77**(4), 046212 (2008)
22. A. Akgul, M. Inc, A. Kilicman, D. Baleanu, A new approach for one-dimensional sine-Gordon equation. **2016**, 8 (2016). https://doi.org/10.1186/s13662-015-0734-x
23. S.W. Goatham, L.E. Mannering, R. Hann, S. Krusch, Acta Phys. Pol. B **42**(10), 2087 (2011)
24. J.A. Gonzalez, A. Bellorín, L.I. Reyes, C. Vasquez, L.E. Guerrero, Geometrical resonance in spatiotemporal systems. Europhys. Lett. **64**(6), 743–749 (2003)
25. J.A. González, S. Cuenda, A. Sánchez, Kink dynamics in spatially inhomogeneous media: the role of internal modes. Phys. Rev. E **75**, 036611 (2007)
26. A.M. Gumerov, E.G. Ekomasov, R.R. Murtzin, V.N. Nazarov, Transformation of sine-Gordon solitons in models with variable coefficients and damping. Comput. Math. Math. Phys. **55**, 628–637 (2015)
27. E.G. Ekomasov, A.M. Gumerov, R.R. Murtazin, Mathematical Methods in the Applied Sciences **40**, 6178 (2016)
28. E.G. Ekomasov, A.M. Gumerov, R.V. Kudryavtsev, JETP Letters 101(12) 835 (2015)
29. E.G. Ekomasov, A.M. Gumerov, R.V. Kudryavtsev, Resonance dynamics of kinks in the sine-Gordon model with impurity, external force and damping. J. Comput. Appl. Math. **312**, 198–208 (2017)
30. J.A. González, A. Bellorín, M.A. García-Ñustes, L.E. Guerrero, S. Jiménez, L. Vázquez, Arbitrarily large numbers of kink internal modes in inhomogeneous sine-Gordon equations. Phys. Lett. A **381**, 1995–1998 (2017)
31. Y.S. Kivshar, D.E. Pelinovsky, Internal Modes of Solitary Waves. Phys. Rev. Lett. **80**(23), 5032–5035 (1998)
32. J.A. González, S. Jiménez, A. Bellorín, L.E. Guerrero, L. Vázquez, Internal degrees of freedom, long-range interactions and nonlocal effects in perturbed Klein–Gordon equations. Physica A **391**, 515–527 (2012)
33. Danial Saadatmand, Sergey V. Dmitriev, Denis I. Borisov, and Panayotis G. Kevrekidi, Physical Review E 90(5), 052902 (2014)
34. T.I. Belova, A.E. Kudryavtsev, Solitons and their interactions in classical field theory. Physics Uspekhi **40**, 359–386 (1997)
35. S.P. Popov, Influence of dislocations on kink solutions of the double sine-Gordon equation. Comput. Math. Math. Phys. **53**, 1891–1899 (2013)
36. E. Zamora-Sillero, N.R. Quintero, F.G. Mertens, Phys. Rev. E **76**, 066601 (2007)
37. A.L. Fabian, R. Kohl, A. Biswas, Perturbation of topological solitons due to sine-Gordon equation and its type. Commun. Nonlinear Sci. Numer. Simul. **14**, 1227–1244 (2009)
38. B.A. Malomed, Dynamics of quasi-one-dimensional kinks in the two-dimensional sine-Gordon model. Physica D: Nonlinear Phenomena **52**, 157–170 (1991)
39. D. Saadatmand, K. Javidan, Collective-coordinate analysis of inhomogeneous nonlinear Klein–Gordon field theory. Braz. J. Phys. **43**(1–2), 48–56 (2013)
40. E.G. Ekomasov, A.M. Gumerov, R.R. Murtazin, R.V. Kudryavtsev, A.E. Ekomasov, N.N. Abakumova, Resonant dynamics of the domain walls in multilayer ferromagnetic structure. Solid State Phenom. **233–234**, 51–54 (2015)
41. E.G. Ekomasov, M.A. Shabalin, Phys. Met. Metallogr. **101**, 48 (2006)
42. E.G. Ekomasov, R.R. Murtazin, O.B. Bogomazova, A.M. Gumerov, One-dimensional dynamics of domain walls in two-layer ferromagnet structure with different parameters of magnetic anisotropy and exchange. J. Magn. Magn. Mater. **339**, 133–137 (2013)
43. E. Ekomasov, R. Murtazin, O. Bogomazova, V. Nazarov, Excitation and dynamics of domain walls in three-layer ferromagnetic structure with different parameters of the magnetic anisotropy and exchange. Mater. Sci. Forum **845**, 195–198 (2016)
44. D.R. Gulevich, F.V. Kusmartsev, Perturbation theory for localized solutions of the sine-Gordon equation: decay of a breather and pinning by a microresistor. Phys. Rev. B **74**, 214303 (2006)
45. L.A. Ferreira, B. Piette, W.J. Zakrzewski, Wobbles and other kink-breather solutions of the sine-Gordon model. Phys. Rev. E **77**, 036616 (2008)
46. G. Kalberman, The sine-Gordon wobble. J. Phys. A Math. Gen. **37**, 11603–11612 (2004)
47. A.M. Gumerov, E.G. Ekomasov, Study of the effect of point defects on the nonlinear dynamics of magnetic nonuniformities. Letters on Materials **3**, 103–105 (2013)
48. A.M. Gumerov, E.G. Ekomasov, F.K. Zakir'yanov, R.V. Kudryavtsev, Structure and properties of four-kink multisolitons of the sine-Gordon equation. Comput. Math. Math. Phys. **54**(3), 491–504 (2014)
49. D. Saadatmand, S.V. Dmitriev, P.G. Kevrekidis, High energy density in multisoliton collisions. Phys. Rev. D **92**, 056005 (2015)
50. D. Saadatmand, S.V. Dmitriev, D.I. Borisov, P.G. Kevrekidis, Interaction of sine-Gordon kinks and breathers with a parity-time-symmetric defect. Phys. Rev. E **90**, 052902 (2014)
51. A.M. Marjaneh, A. Askari, D. Saadatmand, S.V. Dmitriev, Extreme values of elastic strain and energy in sine-Gordon multi-kink collisions. Eur. Phys. J. B **91**, 22 (2018)
52. P.S. Landa, *Nonlinear Oscillations and Waves in Dynamical Systems, Kluwer Academic, Dordrecht (1996)* (Librokom, Moscow, 2010)
53. M.I. Rabinovich, D.I. Trubetskov, *Oscillations and Waves in Linear and Nonlinear Systems, Regulyarnaya I Khaoticheskaya Dinamika, Moscow (2000)* (Kluwer Academic, Dordrecht, 2013)
54. S.P. Popov, Application of the quasi-spectral fourier method to soliton equations. Comput. Math. Math. Phys. **50**(12), 2064–2070 (2010)
55. E.G. Ekomasov, R.K. Salimov, On localized long-lived three-dimensional solutions of the nonlinear Klein-Gordon equation with a fractional power potential. JETP Lett. **100**, 477–480 (2014)
56. A. Mohebbi, M. Dehghan, High-order solution of one-dimensional sine–Gordon equation using compact finite difference and DIRKN methods. Math. and Comp. Modelling **51**(5–6), 537–549 (2010)
57. A.G. Bratsos, The solution of the two-dimensional sine-Gordon equation using the method of lines. J. Comput. Appl. Math. **206**(1), 251–277 (2007)